ORIGINAL PAPER

A novel mathematical model of activation and sensitization of platelets subjected to dynamic stress histories

João S. Soares · Jawaad Sheriff · Danny Bluestein

Abstract Blood recirculating devices, such as ventricular assist devices and prosthetic heart valves, are burdened by thromboembolic complications requiring complex and lifelong anticoagulant therapy with its inherent hemorrhagic risks. Pathologic flow patterns occurring in such devices chronically activate platelets, and the optimization of their thrombogenic performance requires the development of flow-induced platelet activation models. However, existing models are based on empirical correlations using the well-established power law paradigm of constant levels of shear stress during certain exposure times as factors for mechanical platelet activation. These models are limited by their range of application and do not account for other relevant phenomena, such as loading rate dependence and platelet sensitization to high stress conditions, which characterize the dynamic flow conditions in devices. These limitations were addressed by developing a new class of phenomenological stress-induced platelet activation models that specifies the rate of platelet activation as a function of the entire stress history and results in a differential equation that can be directly integrated to calculate the cumulative levels of activation. The proposed model reverts to the power law under constant shear stress conditions and is able to describe experimental results in response to a diverse range of highly dynamic stress conditions found in blood recirculating devices. The model was tested in vitro under emulated device flow conditions and correlates well with experimental results. This new model provides a reliable and robust mathematical tool that can be incorporated into computational fluid dynamic studies in order to optimize design, with the goal of improving the thrombogenic performance of blood recirculating devices.

J. S. Soares · J. Sheriff · D. Bluestein (✉)
Department of Biomedical Engineering, Health Sciences Center,
T15-090, Stony Brook University, Stony Brook, NY 11794-8151, USA
e-mail: danny.bluestein@stonybrook.edu

1 Introduction

The advent of blood recirculating devices and cardiovascular implants (e.g., ventricular assist devices and prosthetic heart valves) has motivated research efforts toward a better understanding of blood damage, hemolysis, and chronic platelet activation induced by such devices (Edmunds 1987; Goldstein 2003). Because of the latter, patients with these classes of implants still develop thromboembolic complications that expose them to a greater risk of cardioembolic stroke and mandate a life-long anticoagulant drug regimen with its inherent risks (Butchart et al. 1988; Wilhelm et al. 1999).

Severely disturbed hemodynamic conditions result from constrictions in blood recirculating devices, and blood flow may become turbulent (Healy et al. 1997). In high-speed rotary ventricular assist devices, platelets are exposed to shear stresses up to 8,000 dyne/cm^2 and extremely high shear stress rates (flow acceleration and deceleration) for durations as short as a few milliseconds (Kini et al. 2001; Cheng et al. 2004; Yoganathan et al. 2004). Such brief durations may still be sufficient to activate platelets (Yin et al. 2005) and additionally sensitize them so that they become substantially more susceptible to further activation in response to subsequent non-pathological shear stresses (Sheriff et al. 2010).

Platelet activation is measured by variety of techniques, traditionally flow cytometry, which quantifies the expression of specific activation markers of receptors on the platelet membrane, for example, P-selectin (a cell adhesion molecule found on the membrane of activated platelets which

interacts with von Willebrand factor and fibrinogen) or Annexin V (a coagulation inhibitor protein that competes with prothrombin for binding sites on the prothrombinase complexes) (Jesty et al. 2003). Other measures of platelet damage include the expression of β-thromboglobulin and lactate dehydrogenase, both being expressed upon platelet lysis (Wurzinger et al. 1985). Other approaches include prothrombinase-based methods and their modifications, representing a more universal measure of platelet contribution to actual coagulation products. A crucial step in platelet activation and the ensuing coagulation cascade is the assembly of prothrombinase complexes in platelet membranes and we have previously developed a modified prothrombinase method called the platelet activation state (PAS) assay (Jesty and Bluestein 1999). Measuring the product of this process—thrombin generation from prothrombin by the prothrombinase complexes—has been thoroughly employed for the determination of platelet activation (Jesty and Bluestein 1999; Jesty et al. 2003; Claiborne et al. 2011).

In order to develop a rational technique to optimize blood recirculating devices with the goal of reducing their thrombogenicity, there is a need to develop reliable models that can predict the damage induced by the pathological regional flow patterns that these devices generate. Platelets, the preeminent cell in thrombosis, respond to mechanical stimuli, as to any other agonist, by a dose–time response (Hellums 1994). Exposure to high mechanical stresses induced by pathological flow conditions characteristic of many prosthetic devices chronically activates platelets and occurs at a shear stress levels an order of magnitude lower than that required for hemolysis (Travis et al. 2001). Models that account for stress-induced platelet activation under the highly dynamic conditions that exist in these devices would allow the direct integration of the biological aspect of platelet activation with in silico approaches to obtain a computational estimation of device thrombogenicity. Device designers could systematically employ cost-effective design optimization techniques instead of the current methodology mostly relying on ad hoc experience (Bluestein et al. 2010).

Limitations in characterizing relevant aspects of the mechanical stimuli and the ability to control them still obscure the physical relationships between mechanical loading and platelet response, hampering our ability to achieve design optimization for blood recirculating devices. Rheological variables related to pulsatility, eddy formation, and turbulence may predominate under many physiological and pathologic conditions (Sutera et al. 1988; Purvis and Giorgio 1991; Merten et al. 2000). In order to predict platelet activation in response to highly dynamic stress histories properly, such phenomena have to be explicitly taken into account. After exposure to sufficiently high shear stresses, platelets do not recover to their pre-exposure activation and instead appear to sensitize, that is, continue to activate at an appreciably greater rate when compared with platelets not primed by prior high shear stress stimuli (Sheriff et al. 2010). In order to capture this sensitization effect, the entire loading history must be taken in account. While we have shown that constant shear stress exposure results in this effect, the role of dynamic conditions (such as flow acceleration and deceleration) is not well understood.

Previous experimental studies have formed the foundation for shear-induced platelet activation occurring due to a combination of either constant exposure time or constant shear stress level (Hellums et al. (1987) and references therein). Empirical models of blood damage or hemolysis are mostly based on these experimental observations; yet, in prosthetic devices, the pathological blood flow patterns that arise are far more dynamic and complicated. The first attempt to associate blood damage/hemolysis with shear stress and exposure time was done by Blackshear et al. (1965), who conducted experiments exposing blood to constant levels of simple shear in a Couette viscometer and approximated their experimental data by means of a power law of the form

$$D = C\tau^{\alpha}t^{\beta}, \tag{1}$$

where D is an index of damage (defined as the percentage of free released hemoglobin indicative of the amount of red blood cell damage/hemolysis), τ is the shear stress, t is the exposure time, and C, α, and β are model coefficients. Following a similar experimental concept, Wurzinger et al. (1985) exposed blood to constant levels of shear stress and measured hemoglobin released from red blood cells (hemolysis) and lactate dehydrogenase from platelets (platelet lysis). Giersiepen et al. (1990) employed the experimental data of Wurzinger et al. (1985) and reduced it into a mathematical correlation of the form of Eq. (1) obtaining $\alpha = 3.075$ and $\beta = 0.77$, demonstrating good agreement and descriptive capabilities within the range of conditions tested. Hellums (1994; Kroll et al. 1996) conducted experiments in which simple shear stress levels were kept constant for varying durations and vice versa, and coined a criterion for the mechanical platelet activation threshold as the locus on the shear stress-exposure time plane (a linear form of Eq. (1) with $\alpha = \beta = 1$ and platelet activation being an all-or-nothing event occurring above a threshold value $A = \tau t$). Boreda et al. (1995) proposed another platelet stimulation function of the power law form which considered $\alpha = 1$ and $\beta = 0.452$ for experimental models of coronary stenosis but did not perform any experimental verification of platelet activation. Jesty et al. (2003) measured the extent of platelet activation in a flow loop using the chemically modified prothrombinase method of Jesty and Bluestein (1999) and corroborated that time of exposure is less significant than the magnitude of shear stress (i.e., $\beta < \alpha$). Grigioni et al. (2005) developed an extension of the power law model to account for piecewise constant shear stress histories, and Nobili et al. (2008) conducted

experiments with platelet mixtures subjected to dynamic shear stress waveforms and measured platelet activation with the prothrombinase assay of Jesty and Bluestein (1999). However, the best fit of their experimental data with the Grigioni et al. (2005) model resulted in $\alpha = 0.6256$ and $\beta = 1.3198$, which contravenes previous results that report the prevalence of shear stress over time of exposure on platelet activation and can be attributed to the highly dynamic nature of their shear stress agonist.

Other platelet activation models have been proposed as possible alternatives of the power law but were not thoroughly followed. Based on damage theories of continuum mechanics, Yeleswarapu et al. (1995) proposed a blood damage model based on a general nonlinear damage equation of the form $\dot{D}(t) = \dot{D}_0 + F(D, \sigma) + \hat{F}(\dot{\sigma})$, where $\dot{D}_0$ represents a constant accumulation of damage, $F(D, \sigma)$ is the contribution due to stress, and $\hat{F}(\dot{\sigma})$ is the contribution of the loading rate. Considering only the second term accounting for damage occurring only due to current level of stress, Yeleswarapu et al. (1995) showed good agreement with constant shear experiments on whole blood and measurements of hemoglobin release. Previously, Ramstack et al. (1979) introduced an empirical model for platelet activation (platelet factor 3 activity) based on a function of shear strain rate γ and a parameter K describing the particular geometry of their experiment. The amount of platelet stimulation (platelet factor 3 activity) was of the form $s = 1 - \exp(-K\gamma t)$, which indeed is a particular solution of an ordinary reaction equation that describes the law of mass action (of the form $ds/dt = K\gamma(1 - s)$, with initial condition $s(0) = 0$, and reaction rate at the origin $K\gamma$).

While power law models generally fitted experimental data where platelets were exposed to constant shear stress levels, they do not address well, if at all, more complicated highly dynamic conditions arising from pathological flow patterns in prosthetic devices. These models appear inadequate to consistently describe the experimental observations of platelet response to highly dynamic stress loading conditions. Nevertheless, the power law model is widely entrenched within the field of computational fluid dynamics (CFD) studies of blood recirculating devices and is faithfully utilized for highly complex and dynamic shear stresses histories, conditions that are clearly outside its range of applicability and verified validity. We propose a novel model based on the specification of the current rate of platelet activation which permits the computation of infinitesimal accumulations as direct summations. This aspect is extremely relevant when one departs from the stringent conditions of empirically derived power laws (constant shear stress for a certain exposure time) to highly dynamic stress histories occurring in blood recirculating devices and considers time as an independent variable. We specify the rate of activation of platelets as a function of their current activation state (i.e., in a

nonlinear process) and stress history (senescence) up to current time. The proposed model is able to capture sensitization due to previous high shear stress activation under subsequent low shear stress conditions, and we are able to properly describe and distinguish different rates of activation under dynamic waveforms due to the explicit inclusion of the contribution of the loading rate platelet activation.

2 Methods

2.1 Shear-induced platelet activation model

In order to address the shortcomings of existing models described above, we present a general model of stress-induced platelet activation in response to dynamic stimuli and incorporate platelet sensitization and loading rate effects. The model is phenomenological in nature and describes the relationship between the loading histories of stress (the model input) and the evolution of platelet activation (the model output).

Platelet activation and damage has been determined with experimental measurements of the expression of several biochemical markers, including β-thromboglobulin, lactate dehydrogenase, Annexin V, thrombin generation, and P-selectin. A crucial step in platelet activation and the ensuing coagulation cascade is the assembly of prothrombinase complexes in platelet membranes, which convert prothrombin into thrombin, and the degree of activation of platelets in a platelet mixture can be determined by assaying the generation of thrombin. We aim for a general model of platelet activation and for that goal we consider a non-dimensional and continuous measure of the degree of platelet activation, the platelet activation state (PAS), defined in the interval PAS $\in\,]0, 1[$. Non-activated quiescent platelets are characterized by PAS $= 0$, whereas the upper bound PAS $= 1$ corresponds to platelets that are fully activated, with each bound representing a situation of either none or all possible prothrombinase complexes being active. The common approach for developing accountable models for mechanical damage/activation of platelets that can be correlated to experiments considers stress as the agonist for platelet activation. The stress tensor is symmetric and composed of six independent components, and a common methodology employed in CFD studies of blood damage relies on the reduction in three-dimensional states of stress into one of its scalar invariants and frame indifference considerations. Bludszuweit (1995a,b) introduced the concept of assigning scalar stress values to path lines representing particle paths through the flow in blood recirculating devices, so that power law models could be employed and predictions readily correlated with the experimental conditions in which most of blood damage tests were conducted. The scalar stress τ at

each location and time of the path line of a fluid particle as it traverses the flow field is obtained by

$$\tau = \left[\frac{1}{6} \sum_{i,j=1}^{3} (\sigma_{ii} - \sigma_{jj})(\sigma_{ii} - \sigma_{jj}) + \sigma_{ij}\sigma_{ij} \right]^{\frac{1}{2}}. \quad (2)$$

where σ_{ij} are the components of the stress tensor. Apel et al. (2001) followed the methodology of Bludszuweit to reduce the tensorial quantity of stress into an easily tractable scalar quantity and interpreted this hypothesis as equating the work done by the fluid in a simple shear flow with the work done on a general three-dimensional deformation. Currently most of the state-of-the-art studies of blood damage or platelet activation in blood recirculating devices employ Eq. (2) with the total stress considered as the summation of viscous and Reynolds stress (cf. Alemu and Bluestein 2007; Wu et al. 2010; Xenos et al. 2010; Girdhar et al. 2012).

A general class of stress-induced platelet activation models is introduced by specifying the rate of platelet activation according to the following formulation

$$\frac{\text{PAS}(t+\Delta t) - \text{PAS}(t)}{\Delta t} \underset{\Delta t \to 0}{=} \frac{\text{dPAS}(t)}{\text{d}t}$$
$$= f[\text{PAS}(t), \tau^{(t)}(s)], \quad (3)$$

where $\tau^{(t)}(s) = \tau(t-s)$, $s \in [0, t]$ is the history of the scalar stress up to time t. We postulate a general nonlinear reaction equation whose rate at current time t depends on the entire stress history and on the current level of activation. With the explicit dependence on PAS, the current rate of activation depends on the current level of activation, that is, platelets with different PAS at time t respond differently to similar stresses. By considering a dependence on the history of stress $\tau^{(t)}(s)$, memory effects due to previous exposures that could impact the current rate at time t are captured. An explicit dependence on stress rate is inherently introduced with the history of this term. Other external variables, such as the presence of activation agonists/inhibitors or platelet count (Schulz-Heik et al. 2005; Sheriff 2010), may play a role, but the scope of this model focuses solely on the effects of stress on platelet activation.

Experimental evidence indicates that platelet activation rate tapers off as activation proceeds, a refractory effect observed both in platelets and in red blood cells (Leverett et al. 1972; Schulz-Heik et al. 2005). Based on a priori theoretical reasoning and the law of mass action of solutions in dynamic equilibrium, the rate of platelet activation at high levels of PAS follows a logistic saturation: as PAS $\to$ 1, dPAS/dt $\to$ 0, that is, as platelets reach maximum activation asymptotically, their activation rate vanishes (because less prothrombinase complexes are available for assembly), and Eq. (3) becomes

$$\frac{\text{dPAS}(t)}{\text{d}t} = K_0[\text{PAS}, \tau^{(t)}(s)](1 - \text{PAS}), \quad (4)$$

where K_0 is interpreted as the rate of stress-induced platelet activation when PAS $= 0$. We further postulate that stress-induced activation is driven by three different and distinctive additive effects of the general form:

$$K_0[\text{PAS}, \tau^{(t)}(s)] = S(\text{PAS}, H_\tau) + F(\text{PAS}, \tau) + G(\text{PAS}, \dot{\tau}). \quad (5)$$

The first term $S(\text{PAS}, H_\tau)$ accounts for platelet sensitization, which is dependent on the current level of activation and explicitly on the stress accumulation of the entire stress history up until time t defined as

$$H_\tau = \int_0^t \tau(s)\text{d}s. \quad (6)$$

The second and third terms, $F(\text{PAS}, \tau)$ and $G(\text{PAS}, \dot{\tau})$, incorporate nonlinear rates of activation which are dependent on the current levels of stress and stress rate. These contributions to the activation rate are nonlinear due to their explicit dependence on PAS, and F and G could be general nonlinear functions of τ and $\dot{\tau}$ accordingly.

Following experimental data of Sheriff et al. (2010), the sensitization response is characterized by the following function:

$$S(\text{PAS}, H_\tau) = S_r \text{PAS} \cdot H_\tau, \quad (7)$$

where S_r is a constant that characterizes the sensitization response. By analyzing experimental data of multiple experiments and attempting different functional relationships for possible correlations, we have found that the rate of sensitization at low levels of activation correlates well with the product of current level of activation and stress accumulation, that is, PAS $\cdot H_\tau$, and a linear relationship adequately describes the experimental data.

The stress level contribution $F(\text{PAS}, \tau)$ is described by the following generalized power law form:

$$F(\text{PAS}, \tau) = C^{\frac{1}{\beta}} \beta \text{PAS}^{\frac{\beta-1}{\beta}} \tau^{\frac{\alpha}{\beta}}, \quad (8)$$

where C, α, and β are constants. This specific form was chosen such that at low levels of activation and under constant shear stress levels, the well-established power law behavior is retained.

In order to characterize the stress rate dependence $G(\text{PAS}, \dot{\tau})$, we propose the following form for its contribution:

$$G(\text{PAS}, \dot{\tau}) = C_r^{\frac{1}{\delta}} \delta \text{PAS}^{\frac{\delta-1}{\delta}} |\dot{\tau}|^{\frac{\gamma}{\delta}}, \quad (9)$$

where C_r, γ, and δ are constants. This particular nonlinear form is consistent with the specific form of Eq. (8). We found this form to confer a proper phenomenological stress rate

effect on platelet activation, which correlates well to previous experimental data.

An initial condition is necessary to obtain particular solutions of Eq. (4): at $t = 0$, the activation level of the platelet mixtures is $PAS(0) = PAS_0$, a value that is measured before each stress loading experiment is performed and represents the initial activation state platelets may have independent of the experiments.

2.2 Platelet activation experiments

We employed a hemodynamic shearing device (HSD) as the test bed for model development and experimental validation. The HSD combines the geometry of a cone and plate viscometer and a cylindrical coaxial Couette viscometer (as shown in Fig. 1) driven by a highly accurate direct motor with very fast dynamic response that is controlled via a programmable interface, as previously described (Girdhar and Bluestein 2008; Xenos et al. 2010; Alemu et al. 2010; Girdhar et al. 2012). The HSD is geometrically designed to generate uniform levels of shear stress throughout the cone-plate and the Couette annular gaps. Assuming that the fluid is Newtonian, only one component of the deviatoric stress tensor is nonzero: the shear stress $\tau = \tau(t)$ that the fluid is subjected to at time t. It is readily observed that the scalar stress resulting from Eq. (2) for simple shear is the shear stress programmed in the HSD. The HSD was operated to generate peak shear stresses up to 70 dyne/cm^2 such that flow remains laminar, inertial effects in the dynamic regime are minimal (time lag until steady state ~0.001 s due to the small cone angle and cylindrical gap), and secondary flow effects are not present (Einav et al. 1994; Girdhar and Bluestein 2008).

Blood was obtained via venipuncture from consenting healthy volunteers of both sexes who had not taken aspirin and ibuprofen at least 2 weeks prior to donation, as per Stony Brook University IRB regulations. Gel-filtered platelets in 2.5 ml of Hepes-modified Tyrodes buffer (20,000 per μL, at 37 °C and with $\mu \approx 1$ cP) were prepared for exposure to shear stress in the HSD as previously described (Sheriff et al. 2010). Platelet activation state (PAS) is measured by the chemically modified prothrombinase method of Jesty and Bluestein (1999). Platelet activation feedback due to generated thrombin is prevented by acetylation of prothrombin, thus establishing a one-to-one correspondence of the rate of acetylated thrombin generation by the activated platelets to the activation agonist, that is, the shear loading (cf. Fig. 2). The assay was extensively shown to correlate extremely well with other methodologies for platelet activation measurement such as Annexin V or P-selectin expression, quantified with flow cytometry (Jesty et al. 2003; Claiborne et al. 2011). Due to the simple shear flow generated by the HSD, the platelet population is uniformly exposed to the same level of shear stress so that PAS is a function of time t only.
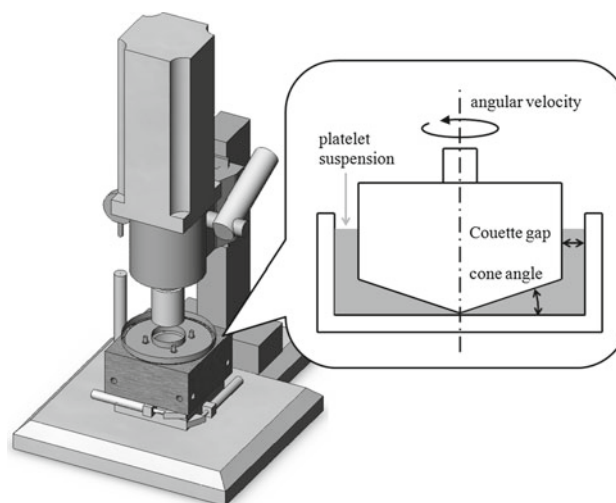

Fig. 1 Schematic of the hemodynamic shearing device (HSD). The HSD combines the geometry of a cone and plate viscometer and a cylindrical coaxial Couette viscometer where the cone angle and the cylinder gap are chosen such that all fluid is subjected to the same level shear stress (schematic not drawn to scale). A highly controllable motor allows the employment of highly dynamic time-dependent shear stress waveforms (adapted with permission from Xenos et al. (2010), Copyright 2010 Elsevier Ltd.)
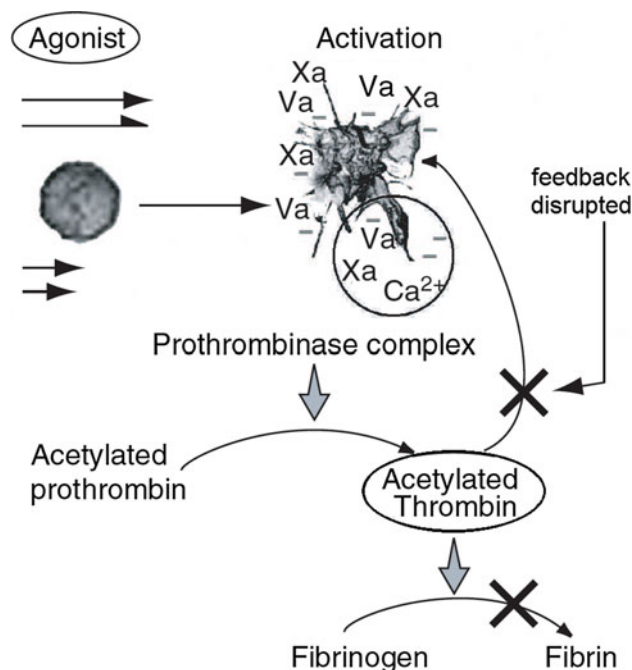

Fig. 2 Platelet activation state (PAS) assay. Acetylated thrombin, which does not contribute to platelet activation in a feedback mechanism, is generated from acetylated prothrombin. In such way, a one-to-one relationship between the activation agonist, shear stress, and acetylated thrombin exists and platelet activation can be reliably measured

Freshly collected non-activated platelet starts with PAS_0, a value measured before each stress loading experiment, and represents the initial activation state of each platelet batch

after it is obtained from subjects, which differ from one individual to another. Due to platelet heterogeneity and donor-to-donor variability, we generally observe $PAS_0 \approx 0$, which corresponds to a mixture of platelets that on average are quiescent (not activated). The upper bound of $PAS = 1$ (maximum activation of a platelet mixture) is obtained with sonication of the platelet mixture, which disrupts platelet membranes and causes total granule release. The measured thrombin conversion of the sonicated mixture is employed to non-dimensionalize the values of thrombin conversion measured with mixtures that were subjected to controlled shear stress histories (cf. Yin et al. 2005).

In the series of experiments employed for model development and validation, the HSD was operated to generate constant and dynamic shear stress loading waveforms or their combinations (Fig. 3):

(a) steps of different magnitude of constant shear stress (10, 30, 50, and 70 dyne/cm^2) for a fixed period of time (2 min, with acceleration and deceleration times of 0.025 s) followed by an extended period of low shear stress (1 dyne/cm^2 up to 14 min);

(b) steps of constant shear stress (30 dyne/cm^2) for different periods of time (1, 2, 3, and 4 min, with acceleration and deceleration times of 0.025 s) followed by an extended period of low shear stress (1dyne/cm^2 up to 14 min);

(c) triangular peaks (of maximum shear stress of 70 dyne/cm^2) of accelerating and decelerating flow with different shear stress rates (ranging from 350 to 2,800 dyne/s cm^2, and all corresponding to equal stress accumulation $H_\tau = 2,800$ dyne · s/cm^2) during 4 min followed by an extended period of low shear stress (1 dyne/cm^2 up to 14 min).

(d) negative control of low constant shear stress (1 dyne/cm^2, with acceleration time of 0.025 s) for 14 min (not shown in Fig. 3).

Samples for activation state measurement were taken from the annular region of the HSD at the start of each experiment ($t = 0$), at intervals of 1 min during high shear loading ($t = 1, 2, 3,$ and 4 min) and every 2.5 min during the subsequent low shear period ($t = 6.5, 9.0, 11.5,$ and 14 min). Platelet counts were taken at the start and at the end to measure any platelet loss. We have conducted 9, 8, and 7 sets of experiments for each type of stress exposure, respectively, and negative control conditions were reproduced for every experimental set to assert its validity.

2.3 Experimental data reduction

We employed the fourth-order Runge–Kutta method to obtain numerical solutions of Eq. (4), that is, the evolution of PAS(t) when subjected to shear stress waveforms $\tau(t)$

(Kincaid and Cheney 2009). A time step of $\Delta t = 0.01$s was employed for all waveforms except for the most dynamic, which required a smaller time step of $\Delta t = 0.005$s in order to properly resolve its peaks. Experimental data reduction to the model constants was performed with the Levenberg–Marquardt method to minimize the least squares error at the experimental observation points (Kincaid and Cheney 2009).

Curve-fitting and the determination of the specific forms of the sensitization, shear stress, and shear stress rate terms in Eq. (4) were performed progressively as follows:

(i) Shear stress term $F(PAS, \tau)$ was obtained by performing data reduction from $t = 0$ to $t = 2$ min and $t = 0$ to $t = 4$ min (3 and 5 experimental data points) with constant shear stress experiments (Fig. 3a and 3b) and the negative control. Constants C, α, and β present in Eq. (8) were determined.

(ii) Shear stress rate term $G(PAS, \dot{\tau})$ was obtained as an additive contribution to the activation rate with data reduction from dynamic shear $t = 0$ to $t = 4$ min (5 experimental data points) with constant shear stress experiments (Fig. 3c). Constants C_r and γ present in Eq. (9) were determined.

(iii) Sensitization term $S(PAS, H_\tau)$ was determined by performing data reduction from the end of the shear loading period, as noted above, to $t = 14$ min with all waveforms and the negative control. Constant S_r present in Eq. (7) was determined.

(iv) A final data reduction encompassing all waveforms and all experimental data points was performed simultaneously with the three terms in Eq. (5), and all constants were tuned one final time.

3 Results

The stress-induced platelet activation model developed shows robust descriptive capability under a diverse range of operating conditions (cf. Figs. 4, 5, 6). Numerical solution of the differential equation (Eq. 4) with the fourth-order Runge–Kutta method results in the temporal evolution of platelet activation state in response to the diverse shear stress conditions employed experimentally (Fig. 3). Experimental data reduction with the Levenberg–Marquardt method results in a set of constants that capture the complex response of platelet activation due to stress stimuli (Eqs. 7–9). With one single set of constants (Table 1), the model is able to properly describe stress-induced platelet activation in response to constant shear stress experiments, either for constant exposure time and different shear stress magnitudes or for constant shear stress magnitudes and different exposure times (Figs. 3a, b, 4, and 5 up to 2 and 4 min, respectively). Under these conditions, predictions of the current model agree well
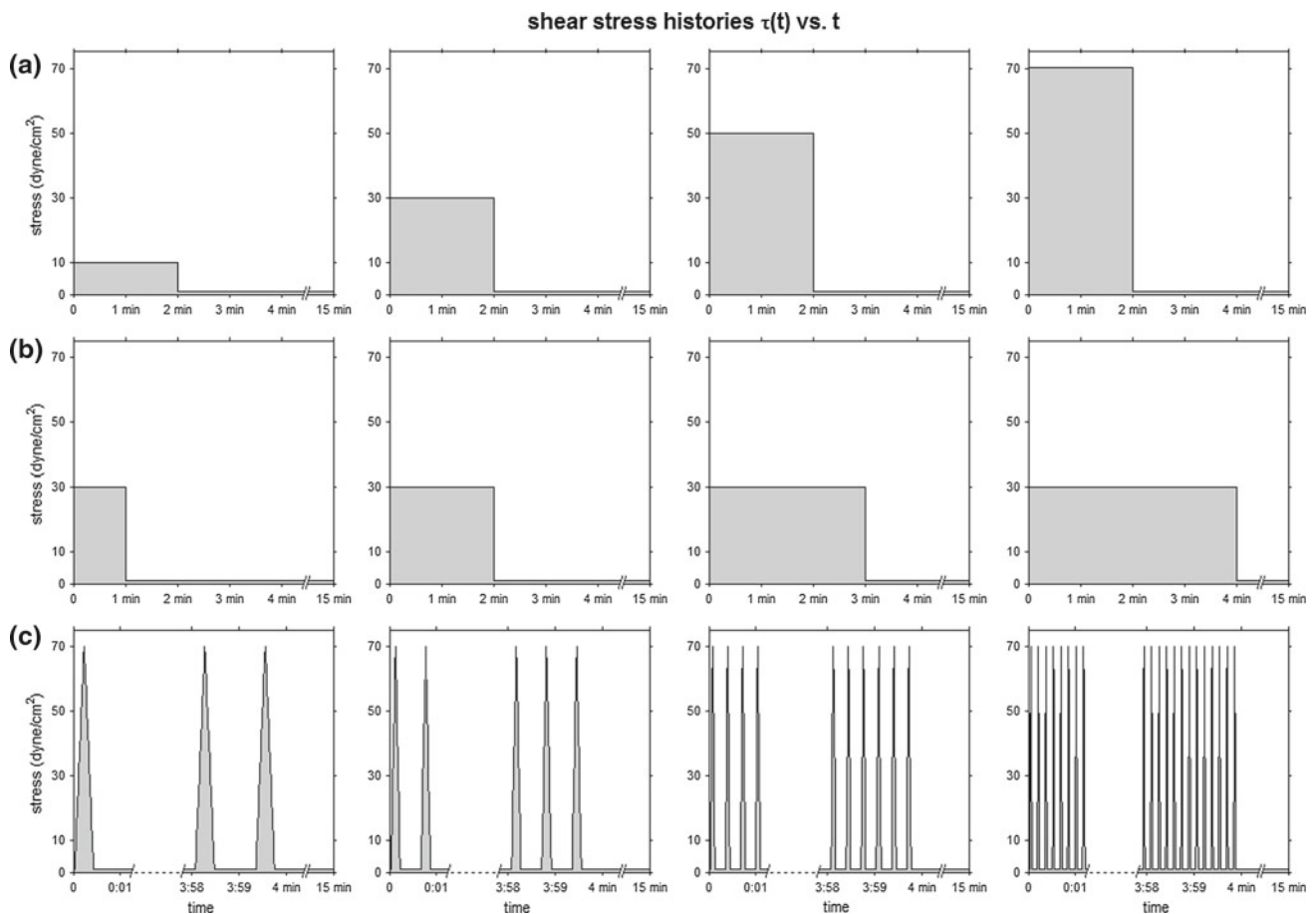
shear stress histories τ(t) vs. t

Fig. 3 Shear stress waveforms programmed to the HSD. Platelets were subjected to high and constant shear stress levels for a certain period of time (up to 4 min) followed by subsequent low shear stress up to 15 min [rows (**a**) and (**b**), respectively]. Highly dynamic waveforms [row (**c**)] were composed of multiple *peaks* of high shear stress at several frequencies up to 4 min followed by a period subsequent low shear stress up to 14 min. Samples were collected at specific time points, and the current state of platelet activation was measured with the PAS assay

with the predictions of the established power law, and in turn, corroborate with the experimental results within this specific range of operation (Table 2).

However, the new model is universal—with the same set of constants defining the process of stress-induced platelet activation, it is able to describe the temporal evolution of platelet activation in response to highly dynamic shear stress experiments (Fig. 6), conditions that are clearly outside of the scope of prior models. Moreover, platelet sensitization occurring after the high shear excitation is also properly described by the nonlinear reaction of the form of Eq. (7). Platelet sensitization rates, defined as rate of increase in activation following shear stress stimuli, were obtained by fitting the experimental measurements during the sensitization period to a line and determining its slope (open squares in Fig. 7). The assumption of sensitization rate as a function of level of activation and stress accumulation holds well for all the experiments considered. The proposed model describes the sensitization behavior occurring after the shear stress stimuli (Figs. 4, 5, 6, after 2 and 4 min, respectively), and Eq. (7) also

results in a good description of sensitization behavior when rate of sensitization is plotted versus the product PAS · H_τ (solid line in Fig. 7).

4 Discussion

We conducted diverse experiments, under constant shear stress conditions as well as under highly dynamic conditions, and corroborated the ability of the power laws model to reasonably fit experimental observations made under constant shear stress conditions (Nobili et al. 2008; Sheriff et al. 2010). However, existing models fail to consistently predict the activation response to both constant shear stress and highly dynamic conditions simultaneously and are naturally unable to describe observable phenomena such as loading rate dependence and sensitization to previous stress histories. These pitfalls raise questions regarding the ability and validity of power law models to describe platelet activation occurring in response to conditions that fall outside of its
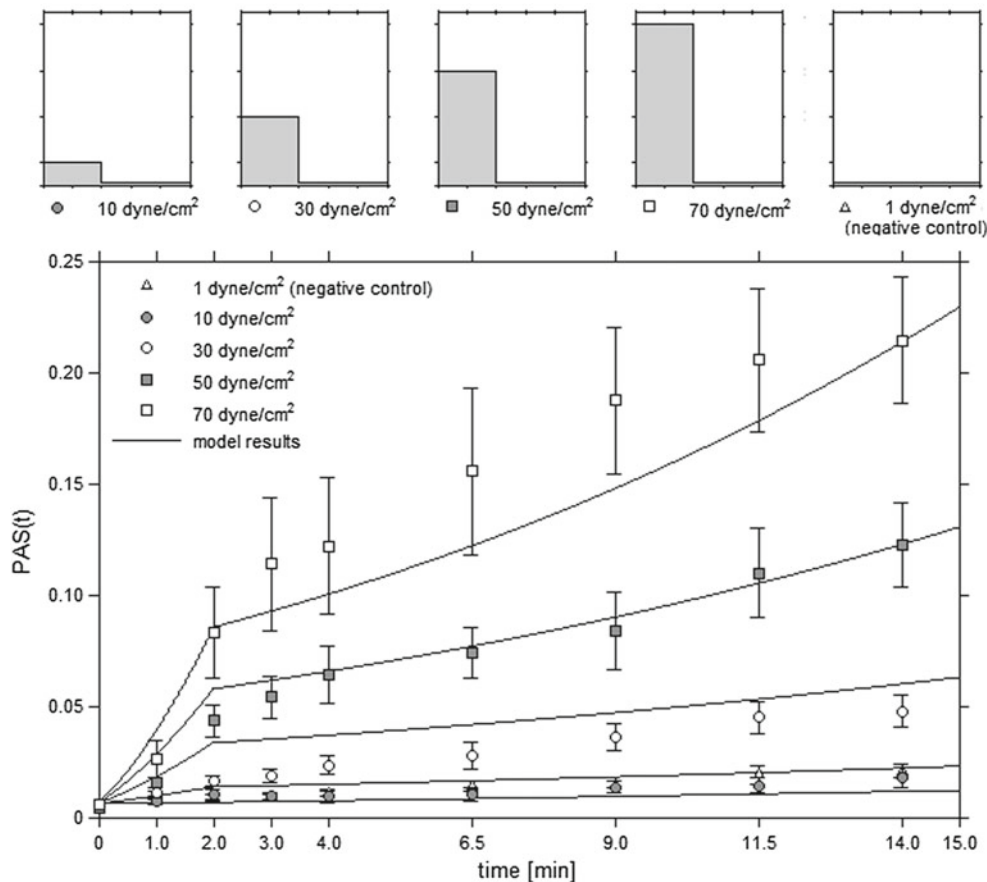
Fig. 4 Evolution of platelet activation in response to different levels of constant shear stress for exposure time of 2 min (*top row*: shear stress waveforms; *markers*: experimentally measured PAS; *lines*: model pre-

diction). Platelet activation occurs due to high shear stress during the initial period of mechanical stimuli, and the proposed model is able to describe activation during constant shear stress (up to 2 min).

initial scope, that is, highly dynamic waveforms. Nevertheless, power law models are widely employed within the field of CFD studies of blood recirculating devices where they are utilized for highly complex and dynamic stresses histories, conditions that are clearly outside their range of applicability.

The nonlinear differential model is based on the specification of the current rate of increase in PAS as a function of the current PAS, and the current mechanical agonist to which platelets are subjected, particularly, the stress and the stress rate (Eq. 3). The current rate of activation is the outcome of three additive contributions: (i) activation due to sensitization to the history (Eq. 7); (ii) activation due to existing levels of stress (Eq. 8), which results in the well-established power law behavior if taken alone under simple shear; and (iii) activation due to existing levels of stress rate (acceleration and deceleration of flow), which vanishes when stress rate is zero (Eq. 9). The ability to describe experimental data under diverse and dynamic conditions with a single set of constants (Figs. 4, 5, 6) offers a significant improvement over existing models.

The inclusion of specific contributions due to sensitization and stress rate allows for the description of platelet activation resulting from highly dynamic shear loading waveforms and the subsequent platelet activation due to prior stimuli.

The power law is a good descriptor of platelet activation, but only for well-defined combinations of constant levels of simple shear for a given exposure durations (Figs. 4, 5; Table 2). With the careful specification of the stress term $F(\text{PAS}, \tau)$ as shown in Eq. (8) with constants $C = 1.4854 \times 10^{-7}$, $\alpha = 1.4854$, and $\beta = 1.4401$, the model reverts to the power law and is able to describe this behavior when subjected to the appropriate conditions (constant levels of simple shear). In fact, when one solely considers the term $F(\text{PAS}, \tau)$ in Eq. (3) and stress constant at all time t, that is, $\tau(t) = \tau_0$, the following ordinary differential equation is obtained

$$\frac{d\text{PAS}(t)}{dt} = C^{\frac{1}{\beta}} \beta \text{PAS}(t)^{\frac{\beta-1}{\beta}} \tau_0^{\frac{\alpha}{\beta}}, \tag{10}$$
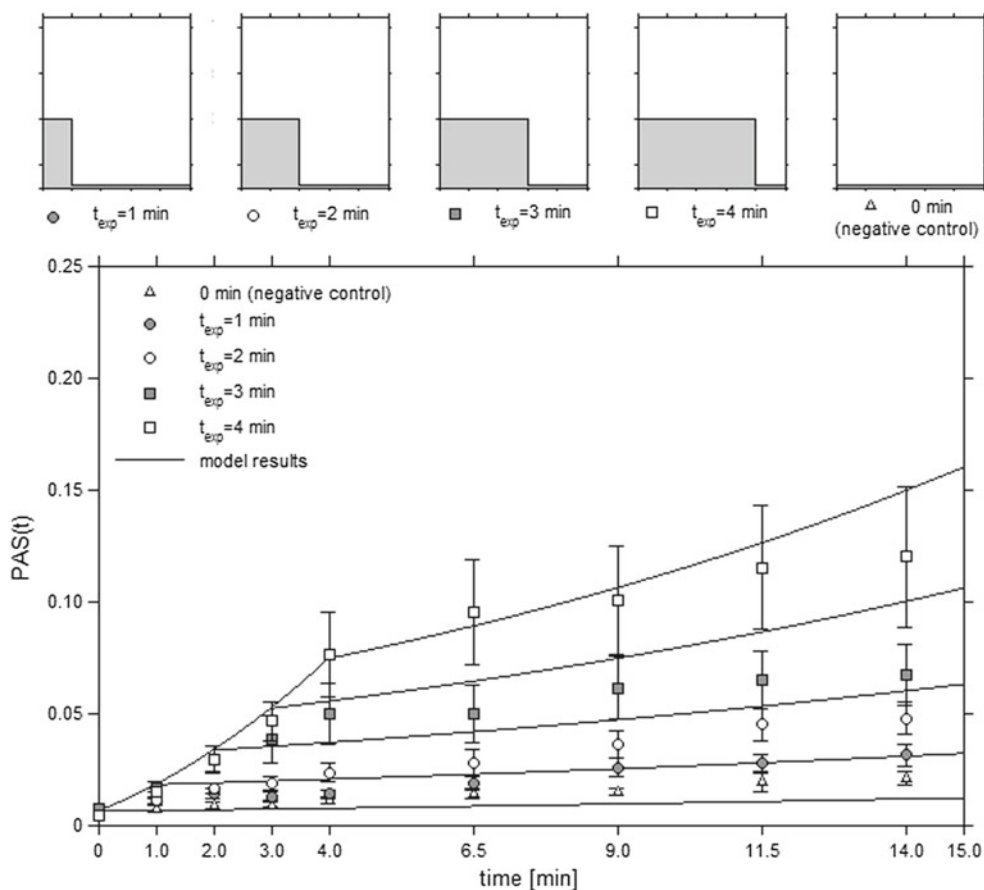
Fig. 5 Evolution of platelet activation in response to different exposure times of constant shear stress of 30 dyne/cm^2 (*top row*: shear stress waveforms; *markers*: experimentally measured PAS; *lines*: model predictions). As in Fig. 4, during the period of mechanical stimuli, platelet activation occurs due to existing level of shear stress. Afterward (up to 14 min), platelets continue to activate at an appreciable rate (although only shear stress of 1 dyne/cm^2 is imposed), and the proposed model captures platelet sensitization

whose general solution is

$$\text{PAS}(t) = \left(C^{\frac{1}{\beta}} \tau_0^{\frac{\alpha}{\beta}} t + C_1 \right)^{\beta} = C \tau_0^{\alpha} t^{\beta} \left(1 + \frac{C_1}{C^{\frac{1}{\beta}} \tau_0^{\frac{\alpha}{\beta}} t} \right)^{\beta},$$

(11)

where C_1 is a constant of integration to be determined by the initial condition. As $\text{PAS}_0 \to 0$ and $\text{PAS}(t) \to C\tau_0^{\alpha} t^{\beta}$—the solution of Eq. (10) is of the specific form of Eq. (1)—and our model reverts to the well-established power law (for constant levels of simple shear, no sensitization, $\text{PAS}_0 \approx 0$ and $\text{PAS} \ll 1$). Alternatively, it can also be easily shown that after expansion, the binomial series of the second term of Eq. (11) converges to unity as t increases.

Activation is significantly different when platelets are subjected to highly dynamic shear stress waveforms (Fig. 3c), even if platelets are exposed to the same stress–time integral. A consistent version of the power law (Eq. 10) is unable to depict these differences properly. In fact, if $\beta = 1$, all these four shear stress histories would lead to the same evolution of PAS, and for $\beta \neq 1$, their differences are still minimal. In order to properly describe this difference in response to dynamic conditions, we introduced $G(\text{PAS}, \dot{\tau})$ (Eq. 9). For consistency but yet sufficient to describe the experimental data (Fig. 6), we considered a nonlinear process that follows a power law behavior on stress rate $\dot{\tau}$ and exposure time with constants $C_r = 1.3889 \times 10^{-4}$, $\gamma = 0.5720$, and $\delta = 0.5125$. Note that whenever the stress rate doubles (as in between the dynamic waveforms depicted in Fig. 3c), the increase in rate of activation does not double. Also, as exposure time increases, the rate decreases, and consequently both exponents are lower than unity.

The significance and consequence of subsequent low shear on platelet activation has not been thoroughly studied, with none of the existing platelet activation models taking platelet sensitization effects into account. The sensitization term is based on our previous experimental
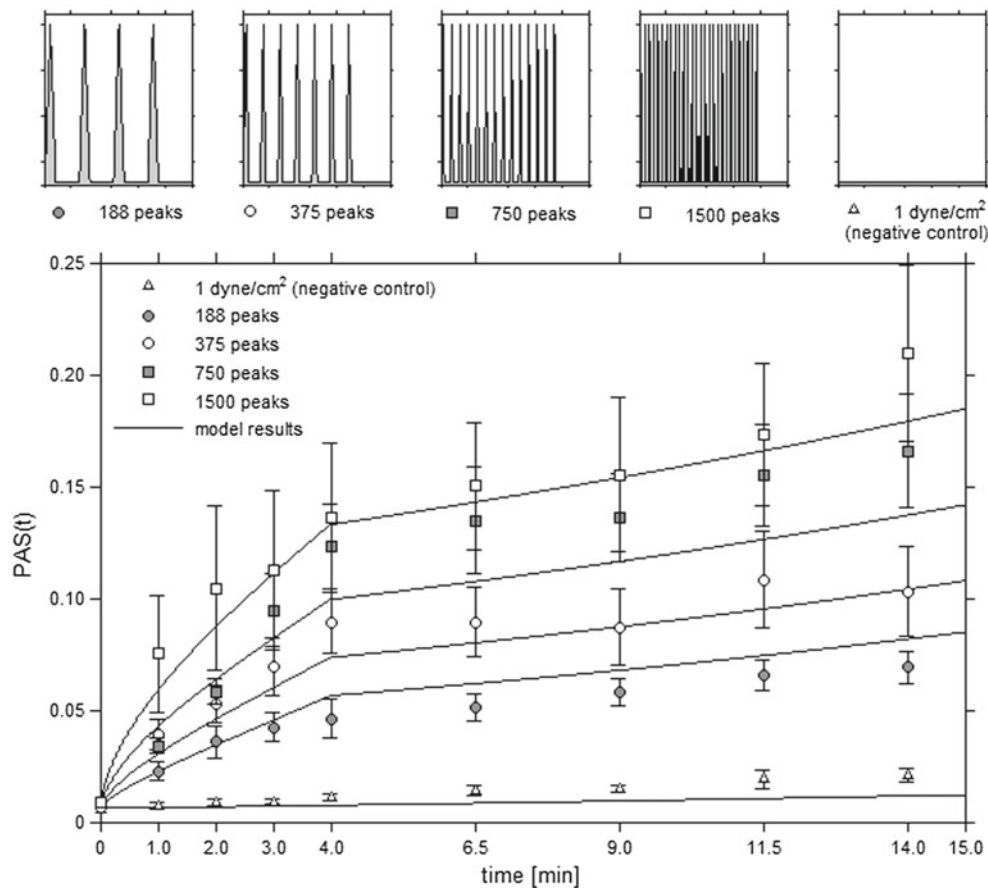
Fig. 6 Evolution of platelet activation in response to different dynamic shear stress waveforms during initial 4 min (*top row*: shear stress waveforms; *markers*: experimentally observed PAS; *lines*: model predictions). Shear stress loading rate plays a role in the rate of platelet activation–platelets exposed to dynamic shear stress histories (triangular waveforms of maximum shear stress of 70 dyne/cm²) show considerable different rates of activation and levels of activation during and after the mechanical stimuli

Table 1 Constants of the model determined by experimental data reduction

S_r	C	α	β	C_r	γ	δ
1.5701×10^{-7}	1.4854×10^{-7}	1.4854	1.4401	1.3889×10^{-4}	0.572	0.5125

observations that platelets primed by high shear stress showed a considerably higher subsequent rate of activation when compared with platelets that were not exposed to such initial high shear stress stimuli (Sheriff et al. 2010). Similar sensitization results were previously observed and reported by Zhang et al. (2002, 2003) in a stenotic flow loop where only the low shear region distal to the high shear in the stenosis contributed to observable significant differences in several activation and aggregation markers. In order to take these effects into account and properly describe the experimental data, we considered a nonlinear mechanism in Eq. (7), such that sensitization rate has an explicit dependence on current level of activation and stress accu-

mulation. We observed good agreement between the specific form of Eq. (7) as a linear function with sensitization constant $S_r = 1.5701 \times 10^{-7}$ and experimental data (Fig. 7). Although the dynamic shear stress waveforms considered (Fig. 3c) have the same amount of stress accumulation, they sensitize platelets at different rates. To properly describe this nonlinear process, the rate of platelet activation and sensitization must depend on current level PAS and on the history of previous stress exposure (senescence): (i) the strongest prior shear stress stimuli result in the most intense sensitization rates (e.g., stress accumulation of 8,400 dyne · s/cm² at 2 min for the most intense constant shear stress waveform in Fig. 3a); (ii) under negligible shear stress, such as the negative

Table 2 Experimental data, power law model, and ODE model predictions for constant shear stress experiments. Experimental data for platelet activation under constant shear stress conditions exhibits a power-law-like behavior. The proposed model shows a similar behavior as it naturally reverts to the power law when constant shear stress experiments are considered and the slight difference arises from the contribution of the sensitization term

Waveform (dyne/cm^2)	Δ PAS (%)					
	$t = 1$ min			$t = 2$ min		
	Experiment[a]	Power law[b]	ODE model[c]	Experiment	Power law	ODE model
1	0.74 ± 0.14	0.37	0.63	0.87 ± 0.13	0.42	0.67
10	0.69 ± 0.13	0.67	0.96	1.03 ± 0.25	1.15	1.36
30	1.06 ± 0.12	1.38	1.80	1.66 ± 0.22	2.89	3.34
50	1.57 ± 0.24	2.10	2.78	4.34 ± 0.71	3.99	5.76
70	2.61 ± 0.84	2.84	3.87	8.31 ± 2.04	6.50	8.53

[a] Experimental data (average $n = 9$) shown in Figs. 4 and 5
[b] Prediction obtained with power law model of Eq. (1) with $C = 1.47 \times 10^{-6}$, $\alpha = 1.04$, $\beta = 1.30$
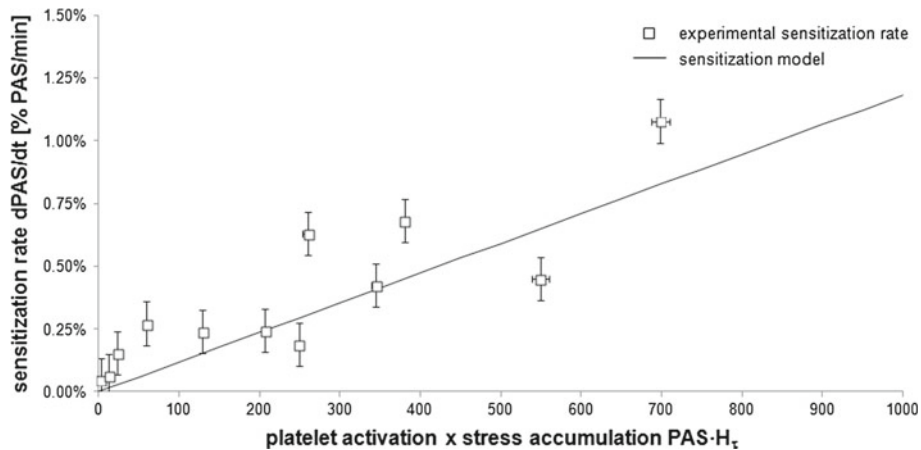[c] Prediction obtained with ODE model of Eq. (3) shown in Figs. 4 and 5

Fig. 7 Rate of platelet sensitization vs. platelet activation level. A correlation is observed between experimentally measured rates of platelet sensitization (y axis) and current levels of platelet activation (x axis) when experimental data are linearized for the period from $t = 4$ min up to $t = 14$ min and averaged for similar stimuli (*open squares*). Model term $S(\text{PAS}, H_\tau)$, shown as the *solid line*, captures this effect

control of 1 dyne/cm^2, PAS evolves with sigmoidal behavior characterized by a very large timescale (not shown); and (iii) without the presence of any shear stress agonist, platelets do not activate and consequently do not sensitize.

4.1 Model input (stress history) and model output (platelet activation state)

One essential issue regarding any stress-induced platelet activation model is determining what stresses are important and how should they be considered. Symmetry of the stress tensor dictates six different and independent components. Fluids are isotropic, with pressure given by one-third of the first invariant of the stress tensor, and the decomposition into volumetric (dilatation) and deviatoric (distortion) components is usually considered. The flow regime is sometimes turbulent, and if so, the Reynolds-averaged Navier–Stokes equations are generally used. The Reynolds stresses, which are the result of the time-averaged formulation of turbulent fluctuations, add to the stress tensor and need turbulence models for closure (such as $k - \varepsilon$ and $k - \omega$ families of models). In the model developed herein, the stress relevant for platelet activation is the stress developed in the HSD. The HSD is controlled with the angular rotation of the cone, and flow remains laminar at the angular speeds considered. With the assumption that the fluid in the HSD behaves as a Newtonian fluid (reasonable assumption taking into consideration that the fluid is Hepes-modified Tyrodes buffer with 0.1 % bovine serum albumin, the only large macromolecule present and a low platelet count of 20,000 per μL), a homogenous state of shear stress is imparted at all regions within the device, that is, the fluid is in simple shear and only one off-diagonal component of the stress tensor is nonzero, with the diagonal components corresponding to the atmospheric pressure. Therefore, with

the reduction in three-dimensional states of stress to a scalar stress (Eq. 2), we developed and validated a scalar model of stress-induced platelet activation, that is, with stress history $\tau^{(t)}(s)$, $s \in [0, t]$ as the input, and the evolution of platelet activation $\mathrm{PAS}(t)$ as the output. However, this reduction in an essentially tensorial quantity into a scalar one represents the introduction of an additional assumption. To illustrate this point, consider the three following stress tensors given by:

$$(\sigma^a) = \begin{pmatrix} -p & \tau_0 & 0 \\ \tau_0 & -p & 0 \\ 0 & 0 & -p \end{pmatrix};$$

$$(\sigma^b) = \begin{pmatrix} -p & \tau_0/\sqrt{2} & \tau/\sqrt{2} \\ \tau_0/\sqrt{2} & -p & 0 \\ \tau_0/\sqrt{2} & 0 & -p \end{pmatrix};$$

$$(\sigma^c) = \begin{pmatrix} -p & \tau_0/\sqrt{3} & \tau_0/\sqrt{3} \\ \tau_0/\sqrt{3} & -p & \tau_0/\sqrt{3} \\ \tau_0/\sqrt{3} & \tau_0/\sqrt{3} & -p \end{pmatrix}$$

Note that in all three cases, their corresponding scalar stress computed with Eq. (2) is rendered to the same $\tau = \tau_0$. Considerable different multidirectional states of stress that result in the same scalar obtained with Eq. (2), which according to Bludszuweit (1995a,b) translate into the same damage/activation, and can (and are most likely to) differ. A fully tensorial model would certainly be advantageous, but would require considerably more complex experimental programs for its validation.

Platelet activation is determined experimentally by assaying thrombin generation. Although freshly collected platelets were subjected to a lifetime of unknown stress histories of non-traumatic stress levels in the vasculature of healthy donors, we generally do not observe any significant platelet activity at time of collection ($\mathrm{PAS}_0 \approx 0$ in all experiments). We consider that stress accumulation occurring previously in vivo is negligible in comparison with the pathological levels of shear stress and stress-rate for long exposure time to which platelets are subjected in vitro. Platelet activation is experimentally bounded with a maximum value of $\mathrm{PAS} = 1$ as determined by the maximum thrombin generation of a sonicated sample used for non-dimensionalization of thrombin generated by sheared platelet mixtures. The range for accurate measurements with the PAS assay should be regarded with care—large noise and loss of accuracy is observed for readings of PAS above 50 % (Joylon Jesty, personal communication, 2012) and experimental data contain a large degree of variability at these levels. Consequently, we are unable to validate the model with sufficient accuracy at such high levels of platelet activation. Nevertheless, based on previous experimental observations and a priori theoretical reasoning, we prescribe that PAS increases asymptotically toward unity following a logistic saturation process (Eq. 4) such that as $\mathrm{PAS} \to 1$, $\mathrm{dPAS}/\mathrm{d}t \to 0$ and the maximum bound of

$\mathrm{PAS} = 1$ is fulfilled. This proves to be extremely useful to consistently employ the proposed model in association with CFD simulations of blood recirculating devices. Other saturation processes, such as Gompertzian, could be similarly incorporated in Eq. (4) for equivalent effect.

4.2 Cumulative platelet activation and time as an independent variable: differential model

By choosing to constitutively specify the rate of activation (Eq. 3), the model is inherently consistent with cumulative contributions by dynamic stress loading histories, allowing one to obtain $\mathrm{PAS}(t + \Delta t) = \mathrm{PAS}(t) + (\mathrm{dPAS}/\mathrm{d}t)\Delta t$ and split dynamic stress waveforms into individual contributions over Δt. This allows computation of $\mathrm{PAS}(t + \Delta t)$ from $\mathrm{PAS}(t)$ by evaluating the rate $\mathrm{dPAS}/\mathrm{d}t$ at time t. Extreme care should be taken when considering such cumulative effects with power law models whenever $\beta \neq 1$ in Eq. (1). Power law formulations originate from empirical observations on a phenomenological basis in order to correlate to measured blood damage, typically under constant shear stress level and exposure time. A model of the differential form with the specification of the platelet activation rate should be preferred whenever one considers time as an independent variable. To illustrate this inconsistency of the power law handling time as an independent variable, consider an initial condition at $t = t_0$ of $\mathrm{PAS}(t_0) = \mathrm{PAS}_0$ subjected to constant shear stress $\bar{\tau}$ during all time t, and two subsequent time points separated by Δt, that is, $t_1 = t_0 + \Delta t$ and $t_2 = t_0 + 2\Delta t$. From Eq. (1) while considering constant shear stress $\bar{\tau}$ and exposure time from t_0 to t_1 and t_2, one obtains respectively:

$$\begin{aligned} \mathrm{PAS}_1 = \mathrm{PAS}(t_1) &= \mathrm{PAS}_0 + C\bar{\tau}^{\alpha}(t_1 - t_0)^{\beta} \\ &= \mathrm{PAS}_0 + C\bar{\tau}^{\alpha}\Delta t^{\beta}, \end{aligned} \tag{12}$$

$$\begin{aligned} \mathrm{PAS}_2 = \mathrm{PAS}(t_2) &= \mathrm{PAS}_0 + C\bar{\tau}^{\alpha}(t_2 - t_0)^{\beta} \\ &= \mathrm{PAS}_0 + C\bar{\tau}^{\alpha}(2\Delta t)^{\beta}. \end{aligned} \tag{13}$$

Alternatively, one could obtain PAS_2 with Eq. (1) with time of exposure from t_1 to t_2, that is,

$$\mathrm{PAS}_2 = \mathrm{PAS}_1 + C\bar{\tau}^{\alpha}(t_2 - t_1)^{\beta} = \mathrm{PAS}_0 + 2C\bar{\tau}^{\alpha}\Delta t^{\beta}, \tag{14}$$

on which, upon substitution of Eq. (12), the inconsistency of the power law formulation is clearly demonstrated as the computed result at t_2 differs (Eqs. 13, 14). Grigioni et al. (2004) showed several inconsistencies with the power law formulation and proposed a modified version of it, but still based on the additive superposition of cumulative damage. A similar argument exposes the same problem (when $\beta \neq 1$) with the modified power law proposed by Grigioni et al. (2005) and later employed by Nobili et al. (2008) and Morbiducci et al. (2009). Goubergrits and Affeld (2004)

recognized the problem arising from the nonlinear dependence on time of exposure and resorted to a cumbersome adaptation to the algebraic methodology for calculating damage from cumulative contributions with Eq. (1) that would resolve the inconsistency observed between Eqs. (13) and (14). They introduced the concept of "virtual time points" between t_1 and t_2 and considered the time of exposure in Eq. (14) as the time from the virtual time point up to t_2 instead of $t_2 - t_1$, such that consistency is force-fitted back into the algebraic model.

In contrast to the algebraic nature of damage models of the form of Eq. (1), the proposed model is based on the specification of the current rate of increase in PAS. In such a way, the cumulative contribution to current PAS due to stress exposure from time t to time $t + \Delta t$ is directly obtained and can be considered as the first-order approximation of a Taylor series expansion at time $t + \Delta t$. If $\beta = 1$, the employment of this argument to result in the power law is quite straightforward (e.g., consider the first-order approximation with $\beta = 1$ in Eq. (10) resulting in $\mathrm{dPAS}/\mathrm{d}t = C\tau^\alpha$). The situation becomes quite problematic in cases when $\beta \neq 1$—one could resort to fractional calculus with non-integer differentiation of order β and the generalized Taylor expansion with Caputo fractional derivatives (Odibat and Shawagfeh 2007), but such mathematical analysis is unnecessarily complex and other strategies, such as presented in this study, prove to be more reasonable and cost-effective. The crux of our argument is that cumulative damage cannot be consistently computed as an algebraic summation of infinitesimal contributions with Eq. (1) whenever the power on time β is not equal to 1. Instead, integration of differential equations specifying the current rate (such as Eqs. (4) or (10)) should be preferred, with the goal of obtaining consistent models which agree with the experimental observations that were the origin of the power law.

This problematic aspect of the power law formulation becomes extremely relevant when one employs cumulative summations of platelet activation or blood damage under highly dynamic stresses with $\tau = \tau(t)$ and t as an independent variable. This methodology is usually followed in CFD studies of blood flow in recirculating devices for thrombogenic optimization (Bluestein et al. 1997, 2002; Yin et al. 2004). Stress histories were initially obtained along trajectories of the complex flow fields that originate around these devices and resolved with CFD techniques, and the current state of the art is to employ two-phase fluid models (fluid with discrete particles that simulate platelets) to compute the stress histories along particle trajectories (Tambasco and Steinman 2003; Song et al. 2003; Dumont et al. 2007; Alemu et al. 2010; Xenos et al. 2010; Girdhar et al. 2012; Yun et al. 2012). This approach certainly leads to a very accurate and detailed analysis of the stress histories that individual platelets experience as they flow through a medical

device and allows the calculation of damage accumulation computed along its trajectory. Nevertheless, damage accumulation computed with algebraic power law models of the form of Eq. (1) is inconsistent if $\beta \neq 1$ (as considered by Song et al. (2003), Wu et al. (2005, 2010), Morbiducci et al. (2009)), and as expected, cannot describe the phenomenon of platelet sensitization and does not account for the full effect of the dynamic stress rates occurring in blood recirculating devices.

4.3 Limitations

Limitations of the new model may reside in its range of verified validity and its assumptions, which are inherent to any modeling of such complex biological response. The in vitro experimental conditions are idealized and may not fully represent typical extreme flow conditions in devices, in particular, multi-dimensional states of stress. Similar to previous mechanistic models of blood damage, the fundamental model assumption asserts that stress is the dominant factor for platelet activation and three-dimensional states of stress can be reduced to a scalar counterpart, and for such, our experimental apparatus is highly appropriate. The HSD was operated at a range of 70 dyne/cm^2 and below to guarantee shear stress uniformity, while shear stress levels in actual blood recirculating devices may exceed this level. Thus, sufficient care should be reserved when considering stimuli outside the range of experimental validation. However, stress-induced platelet activation is systematically observed under these conditions and such process is properly described by our model.

5 Conclusions

We put forth a general class of stress-induced platelet activation models of the differential type based on a general reaction equation. The model is phenomenological and builds upon previously existing shear-induced platelet activation models and successfully describes experimental observations of platelet response to a variety of dynamic shear stress conditions. It is able to address inconsistencies associated with previous models under such conditions. This class of models produces a better description and estimation of the phenomena of stress-induced platelet activation in a much broader range of operating conditions, such as response to highly dynamic stress stimuli, and properly describes the phenomena of platelet sensitization. The incorporation of an accountable model for platelet activation under dynamic stress loading conditions with strong descriptive capabilities in CFD codes would allow for better estimation and optimization of platelet activation occurring in blood recirculating

devices in silico for achieving optimization of their thromboresistance during the design stage.

References

Alemu Y, Bluestein D (2007) Flow-induced platelet activation and damage accumulation in a mechanical heart valve: numerical studies. Artif Organs 31(9):677–688

Alemu Y, Girdhar G, Xenos M, Sheriff J, Jesty J, Einav S, Bluestein D (2010) Design optimization of a mechanical heart valve for reducing valve thrombogenicity–a case study with ats valve. ASAIO J 56(5):389–396

Apel J, Paul R, Klaus S, Siess T, Reul H (2001) Assessment of hemolysis related quantities in a microaxial blood pump by computational fluid dynamics. Artif Organs 25(5):341–347

Blackshear PL, Dorman FD, Steinbach JH (1965) Some mechanical effects that influence hemolysis. Trans Am Soc Artif Int Organs 11:112–117

Bludszuweit C (1995a) Model for a general mechanical blood damage prediction. Artif Organs 19(7):583–589

Bludszuweit C (1995b) Three-dimensional numerical prediction of stress loading of blood particles in a centrifugal pump. Artif Organs 19(7):590–596

Bluestein D, Chandran KB, Manning KB (2010) Towards non-thrombogenic performance of blood recirculating devices. Ann Biomed Eng 38(3):1236–1256

Bluestein D, Li YM, Krukenkamp IB (2002) Free emboli formation in the wake of bi-leaflet mechanical heart valves and the effects of implantation techniques. J Biomech 35(12):1533–1540

Bluestein D, Niu L, Schoephoerster RT, Dewanjee MK (1997) Fluid mechanics of arterial stenosis: relationship to the development of mural thrombus. Ann Biomed Eng 25(2):344–356

Boreda R, Fatemi RS, Rittgers SE (1995) Potential for platelet stimulation in critically stenosed carotid and coronary arteries. J Vasc Inv 1:26–37

Butchart EG, Lewis PA, Grunkemeier GL, Kulatilake N, Breckenridge IM (1988) Low risk of thrombosis and serious embolic events despite low-intensity anticoagulation. Experience with 1,004 medtronic hall valves. Circulation 78(3 Pt 2):I66–I77

Cheng R, Lai YG, Chandran KB (2004) Three-dimensional fluid-structure interaction simulation of bileaflet mechanical heart valve flow dynamics. Ann Biomed Eng 32(11):1471–1483

Claiborne TE, Girdhar G, Gallocher-Lowe S, Sheriff J, Kato YP, Pinchuk L, Schoephoerster RT, Jesty J, Bluestein D (2011) Thrombogenic potential of innovia polymer valves versus carpentier-edwards perimount magna aortic bioprosthetic valves. ASAIO J 57(1):26–31

Dumont K, Vierendeels J, Kaminsky R, Van Nooten G, Verdonck P, Bluestein D (2007) Comparison of the hemodynamic and thrombogenic performance of two bileaflet mechanical heart valves using a cfd/fsi model. J Biomech Eng-T ASME 129(4):558–565

Edmunds LH Jr (1987) Thrombotic and bleeding complications of prosthetic heart valves. Ann Thorac Surg 44(4):430–445

Einav S, Dewey CF, Hartenbaum H (1994) Cone-and-plate apparatus–a compact system for studying well-characterized turbulent-flow fields. Exp Fluids 16(3–4):196–202

Giersiepen M, Wurzinger LJ, Opitz R, Reul H (1990) Estimation of shear stress-related blood damage in heart-valve prostheses–in vitro comparison of 25 aortic valves. Int J Artif Organs 13(5):300–306

Girdhar G, Bluestein D (2008) Biological effects of dynamic shear stress in cardiovascular pathologies and devices. Expert Rev Med Devices 5(2):167–181

Girdhar G, Xenos M, Alemu Y, Chiu WC, Lynch BE, Jesty J, Einav S, Slepian MJ, Bluestein D (2012) Device thrombogenicity emulation: a novel method for optimizing mechanical circulatory support device thromboresistance. PLoS One 7(3):e32463

Goldstein DJ (2003) Worldwide experience with the micromed debakey ventricular assist device (r) as a bridge to transplantation. Circulation 108(10):272–277

Goubergrits L, Affeld K (2004) Numerical estimation of blood damage in artificial organs. Artif Organs 28(5):499–507

Grigioni M, Daniele C, Morbiducci U, D'Avenio G, Benedetto GD, Barbaro V (2004) The power-law mathematical model for blood damage prediction: analytical developments and physical inconsistencies, Artif Organs 28(5):467–475

Grigioni M, Morbiducci U, D'Avenio G, Benedetto GD, Gaudio CD (2005) A novel formulation for blood trauma prediction by a modified power-law mathematical model. Biomech Model Mechanobiol 4(4):249–260

Healy TM, Ellis JT, Fontaine AA, Jarrett CA, Yoganathan AP (1997) An automated method for analysis and visualization of laser doppler velocimetry data. Ann Biomed Eng 25(2):335–343

Hellums JD (1994) 1993 whitaker lecture: biorheology in thrombosis research. Ann Biomed Eng 22(5):445–455

Hellums JD, Peterson DM, Stathopoulos NA, Moake JL, Giorgio TD (1987) Studies on the mechanisms of shear-induced platelet activation. In: Hartman A, Kuschinsky W (eds) Cerebral ischemia and hemorheology. Springer, New York, pp 80–89

Jesty J, Bluestein D (1999) Acetylated prothrombin as a substrate in the measurement of the procoagulant activity of platelets: elimination of the feedback activation of platelets by thrombin. Anal Biochem 272(1):64–70

Jesty J, Yin W, Perrotta P, Bluestein D (2003) Platelet activation in a circulating flow loop: combined effects of shear stress and exposure time. Platelets 14(3):143–149

Kincaid D, Cheney EW (2009) Numerical analysis : mathematics of scientific computing. The sally series, vol 2, 3rd edn. American Mathematical Society, Providence, RI

Kini V, Bachmann C, Fontaine A, Deutsch S, Tarbell JM (2001) Integrating particle image velocimetry and laser doppler velocimetry measurements of the regurgitant flow field past mechanical heart valves. Artif Organs 25(2):136–145

Kroll MH, Hellums JD, McIntire LV, Schafer AI, Moake JL (1996) Platelets and shear stress. Blood 88(5):1525–1541

Leverett LB, Hellums JD, Alfrey CP, Lynch EC (1972) Red blood cell damage by shear stress. Biophys J 12(3):257–273

Merten M, Chow T, Hellums JD, Thiagarajan P (2000) A new role for p-selectin in shear-induced platelet aggregation. Circulation 102(17):2045–2050

Morbiducci U, Ponzini R, Nobili M, Massai D, Montevecchi FM, Bluestein D, Redaelli A (2009) Blood damage safety of prosthetic heart valves. Shear-induced platelet activation and local flow dynamics: a fluid-structure interaction approach. J Biomech 42(12):1952–1960

Nobili M, Sheriff J, Morbiducci U, Redaelli A, Bluestein D (2008) Platelet activation due to hemodynamic shear stresses: damage accumulation model and comparison to in vitro measurements. ASAIO J 54(1):64–72

Odibat ZM, Shawagfeh NT (2007) Generalized taylor's formula. Appl Math Comput 186(1):286–293

Purvis NB Jr, Giorgio TD (1991) The effects of elongational stress exposure on the activation and aggregation of blood platelets. Biorheology 28(5):355–367

Ramachandran J, Rubenstein D, Bluestein D, Jesty J (2004) Activation of platelets exposed to shear stress in the presence of smoke extracts

of low-nicotine and zero-nicotine cigarettes: the protective effect of nicotine. Nicotine Tob Res 6(5):835–841

Ramstack JM, Zuckerman L, Mockros LF (1979) Shear-induced activation of platelets. J Biomech 12(2):113–125

Schulz-Heik K, Ramachandran J, Bluestein D, Jesty J (2005) The extent of platelet activation under shear depends on platelet count: differential expression of anionic phospholipid and factor va. Pathophysiol Haemost Thromb 34(6):255–262

Sheriff J (2010) Shear-induced platelet sensitization and the development of an activation model. Stony Brook University, Stony Brook

Sheriff J, Bluestein D, Girdhar G, Jesty J (2010) High-shear stress sensitizes platelets to subsequent low-shear conditions. Ann Biomed Eng 38(4):1442–1450

Song X, Throckmorton AL, Wood HG, Antaki JF, Olsen DB (2003) Computational fluid dynamics prediction of blood damage in a centrifugal pump. Artif Organs 27(10):938–941

Sutera SP, Nowak MD, Joist JH, Zeffren DJ, Bauman JE (1988) A programmable, computer-controlled cone-plate viscometer for the application of pulsatile shear stress to platelet suspensions. Biorheology 25(3):449–459

Tambasco M, Steinman DA (2003) Path-dependent hemodynamics of the stenosed carotid bifurcation. Ann Biomed Eng 31(9):1054–1065

Travis BR, Marzec UM, Ellis JT, Davoodi P, Momin T, Hanson SR, Harker LA, Yoganathan AP (2001) The sensitivity of indicators of thrombosis initiation to a bileaflet prosthesis leakage stimulus. J Heart Valve Dis 10(2):228–238

Wilhelm CR, Ristich J, Knepper LE, Holubkov R, Wisniewski SR, Kormos RL, Wagner WR (1999) Measurement of hemostatic indexes in conjunction with transcranial doppler sonography in patients with ventricular assist devices. Stroke 30(12):2554–2561

Wu J, Antaki JF, Snyder TA, Wagner WR, Borovetz HS, Paden BE (2005) Design optimization of blood shearing instrument by computational fluid dynamics. Artif Organs 29(6):482–489

Wu J, Paden BE, Borovetz HS, Antaki JF (2010) Computational fluid dynamics analysis of blade tip clearances on hemodynamic performance and blood damage in a centrifugal ventricular assist device. Artif Organs 34(5):402–411

Wurzinger LJ, Opitz R, Blasberg P, Schmid-Schonbein H (1985) Platelet and coagulation parameters following millisecond exposure to laminar shear stress. Thromb Haemost 54(2):381–386

Xenos M, Girdhar G, Alemu Y, Jesty J, Slepian M, Einav S, Bluestein D (2010) Device thrombogenicity emulator (dte)-design optimization methodology for cardiovascular devices: a study in two bileaflet MHV designs. J Biomech 43(12):2400–2409

Yeleswarapu KK, Antaki JF, Kameneva MV, Rajagopal KR (1995) A mathematical model for shear-induced hemolysis. Artif Organs 19(7):576–582

Yin W, Alemu Y, Affeld K, Jesty J, Bluestein D (2004) Flow-induced platelet activation in bileaflet and monoleaflet mechanical heart valves. Ann Biomed Eng 32(8):1058–1066

Yin W, Gallocher S, Pinchuk L, Schoephoerster RT, Jesty J, Bluestein D (2005) Flow-induced platelet activation in a st. Jude mechanical heart valve, a trileaflet polymeric heart valve, and a St. Jude tissue valve. Artif Organs 29(10):826–831

Yoganathan AP, He Z, Casey Jones S (2004) Fluid mechanics of heart valves. Annu Rev Biomed Eng 6:331–362

Yun BM, Wu J, Simon HA, Arjunon S, Sotiropoulos F, Aidun CK, Yoganathan AP (2012) A numerical investigation of blood damage in the hinge area of aortic bileaflet mechanical heart valves during the leakage phase. Ann Biomed Eng 40(7):1468–1485

Zhang JN, Bergeron AL, Yu Q, Sun C, McIntire LV, Lopez JA, Dong JF (2002) Platelet aggregation and activation under complex patterns of shear stress. Thromb Haemost 88(5):817–821

Zhang JN, Bergeron AL, Yu QH, Sun C, McBride L, Bray PF, Dong JF (2003) Duration of exposure to high fluid shear stress is critical in shear-induced platelet activation-aggregation. Thromb Haemost 90(4):672–678